TERAHERTZ SPECTROSCOPIC INVESTIGATION OF SALICYLIC ACID AND SODIUM SALICYLATE**

L. Ding [1,2], W.-H. Fan [1*], C. Song [1,2], X. Chen [1,2], Z.-Y. Chen [1,2]

[1] State Key Laboratory of Transient Optics and Photonics, Xi'an Institute of Optics and Precision Mechanics, Chinese Academy of Sciences, Xi'an 710119, China; e-mail: fanwh@opt.ac.cn
[2] University of Chinese Academy of Sciences, Beijing 100049, China

The terahertz spectra of salicylic acid and sodium salicylate are measured by broadband terahertz time-domain spectroscopy (THz-TDS). Two absorption features of salicylic acid and three characteristic features of sodium salicylate are reported for the first time. Our investigation shows that salicylic acid and sodium salicylate can be easily distinguished based on their distinctive THz spectra, which could be attributed to their intra- and intermolecular structure differences. Furthermore, solid-state density functional theory calculations reveal that the absorption features of salicylic acid mainly originate from intermolecular interactions, except the absorption feature at 2.28 THz, while gaseous-state theory calculations show that the absorption features of sodium salicylate mainly come from intramolecular vibrations except the absorption feature at 0.40 THz. Our investigation indicates that THz vibrational modes are highly sensitive to molecular structures and intermolecular interactions, promoting the application of THz spectroscopy in distinguishing chemicals and pharmaceuticals with similar molecular structures.

Keywords: *terahertz spectrum, density functional theory, intermolecular interactions, intramolecular vibrations.*

ТЕРАГЕРЦОВОЕ СПЕКТРОСКОПИЧЕСКОЕ ИССЛЕДОВАНИЕ САЛИЦИЛОВОЙ КИСЛОТЫ И САЛИЦИЛАТА НАТРИЯ

L. Ding [1,2], W.-H. Fan [1*], C. Song [1,2], X. Chen [1,2], Z.-Y. Chen [1,2]

УДК 539.194:547.587.11

[1] Сианьский институт оптики и точной механики Китайской АН, Сиань, 710119, Китай; e-mail: fanwh@opt.ac.cn
[2] Университет Китайской АН, Пекин 100049, Китай

(Поступила 18 сентября 2017)

Терагерцовые спектры салициловой кислоты и салицилата натрия измерены методом широкополосной терагерцовой спектроскопии с временным разрешением. Установлены новые особенности поглощения салициловой кислоты и салицилата натрия. Показано, что салициловую кислоту и салицилат натрия можно легко различать на основе их терагерцовых спектров, что связано с их внутри- и межмолекулярными структурными различиями. Расчеты в соответствии с теорией функционала плотности твердого тела свидетельствуют о том, что особенности поглощения салициловой кислоты (за исключением 2.28 ТГц) обусловлены в основном межмолекулярными взаимодействиями. Согласно расчетам в соответствии с теорией газов поглощение салицилата натрия (за исключением 0.40 ТГц) обусловлено главным образом внутримолекулярными вибрациями. Установлено, что колебательные терагерцовые моды высокочувствительны к молекулярной структуре и межмолекулярным взаимодействиям. Это способствует применению терагерцовой спектроскопии для идентификации химических веществ и лекарственных препаратов со сходной молекулярной структурой.

Ключевые слова: *терагерцовый спектр, теория функционала плотности, межмолекулярные взаимодействия, внутримолекулярные колебания.*

** Full text is published in JAS V. 85, No. 6 (http://springer.com/10812) and in electronic version of ZhPS V. 85, No. 6 (http://www.elibrary.ru/title_about.asp?id=7318; sales@elibrary.ru).

Introduction. Terahertz (THz) spectroscopy, ranging from 0.1–10 THz, has received increasing attention in numerous applications, including identification of drugs and explosives [1, 2], characterization of biological organics [3–5], and analysis of mixtures [6, 7]. These applications are based on the fact that THz spectroscopy is highly sensitive to molecular structures and intermolecular interactions, which allows it to be utilized in distinguishing chemicals and pharmaceuticals with similar molecular structures [8–10].

It is well known that salicylic acid and sodium salicylate have similar molecular structures, since the main difference between their molecular structures is that the hydrogen atom in the carboxyl group of salicylic acid is replaced by the sodium atom in the carboxyl group of sodium salicylate. As a result, their applications vary greatly in spite of their similar appearance. Salicylic acid, a natural antibiotic medicine, plays an important role in treating various chronic skin diseases, while sodium salicylate is popular for treating active rheumatism, rheumatoid arthritis, and acute embolism. Due to their different applications, it is vital to distinguish them by investigating their characteristic THz spectra. Although the THz spectra of salicylic acid have been widely investigated [11–15], few studies on the THz spectrum of sodium salicylate have been reported so far. Hisazumi et al. [16] reported merely one absorption feature of sodium salicylate at 0.40 THz under 2.0 THz, but no further theoretical explanation has been made to date. Therefore, further investigation on salicylic acid and sodium salicylate combining THz spectroscopy with theoretical calculation is critically important.

In this paper, the THz absorption spectra of salicylic acid and sodium salicylate have been measured by THz time-domain spectroscopy (THz-TDS) from 0.1 to 3.6 THz with a spectral resolution of 0.03 THz. Two absorption features of salicylic acid as well as three characteristic features of sodium salicylate are reported for the first time. Sodium salicylate exhibits very different THz absorption features compared with salicylic acid, which could be attributed to their different intra- and intermolecular interactions. Furthermore, the vibrational modes corresponding to the measured THz features of salicylic acid and sodium salicylate are analyzed based on theoretical calculations, and the understanding of these THz features is achieved.

Experimental. Salicylic acid (CAS-number 69-72-7) and sodium salicylate (CAS-number 54-21-7) were purchased from Tianjin Jinbeichem Co. Ltd. The two samples are in analytical reagent (>99.5%) and directly used without further purification. In order to minimize particle scattering, both samples were first ground into fine powder with a pestle and mortar. After that, these two samples were pressed into 0.50-mm-thick pellets with a diameter of 13 mm under a pressure of 400 kg/cm^2 for measurements.

Experimental apparatus and data processing. THz absorption spectra of salicylic acid and sodium salicylate were measured using a TeraView TPS 3000 spectrometer from 0.1 to 3.6 THz with a spectral resolution of 0.03 THz. In the spectrometer, a laser beam with an average power of 300 mW and a pulse duration of 80 fs was first split into a pump beam and a probe beam by a beam splitter for generation and detection of THz pulses, respectively. The THz radiation was generated by a photoconductive antenna excited by the pump beam and then collimated and focused on the sample by a pair of off-axis parabolic mirrors (OAPMs). After transmitting through the sample, the THz radiation was detected by another photoconductive antenna gated by the probe beam. By varying the optical delay between the probe beam and the pump beam, both phase and amplitude of time-domain spectra were obtained. Furthermore, to improve the signal-to-noise ratio, all the samples and blank references were scanned 1800 times and the spectral data were the averages of these data sets. Finally, the THz spectra were acquired by applying Fast Fourier Transform (FFT) to the time-domain waveforms, and the absorption spectrum of each sample was proportional to the log-ratio of the sample spectrum and the reference spectrum. Moreover, to minimize the water vapor absorption, all the measurements were carried out in dry air (relative humidity<1%).

Theoretical methods. For salicylic acid, calculations based on the periodic system were carried out using the plane-wave density functional theory (DFT) with generalized gradient approximation (GGA) [17]. The Perdew–Burke–Ernzerhof (PBE) exchange correlation functional [18] was used in simulations, since this functional can produce high-quality simulations of solid-state structures and THz spectra [19, 20]. The Tkatchenko–Scheffler method [21] was applied to correct long-range dispersion interactions, and normal-conserving Kleinman–Bylander pseudopotentials [22] were employed to describe electron–ion interactions. The relevant calculation parameters were used as follows: Brillouin zone integrations were conducted using a Monkhorst–Pack *k*-point mesh [23] with 0.05 Å^{-1} intervals; the plane-wave cutoff energy was 1200 eV; the total energy of the system was converged to 10^{-8} eV/atom, and the forces on an atom were reduced to lower than 10^{-4} eV/Å. After geometry optimization, the frequencies and infrared intensities of the vibrational modes at the Γ-point were calculated at given normal-mode eigenvectors and effective charges. All the calculations were performed in the fixed unit cell. The crystal cell parameters of salicylic acid were as follows [24]: space

group $P21/a$, $Z = 4$, $a = 11.52$ Å, $b = 11.21$ Å, $c = 4.92$ Å, $\alpha, \gamma = 90.00°$, $\beta = 90.83°$. Also, based on crystallographic structure analysis, salicylic acid molecules form a centrosymmetric dimer, as illustrated in Fig. 1.

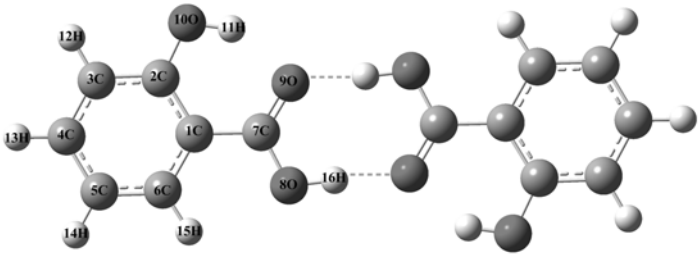

Fig. 1. The centrosymmetric dimeric structure and atom labeling of salicylic acid.

As for sodium salicylate, calculations based on isolated-molecule were performed using the gaseous-state theory with the linear combination of the atomic orbital method, because there are no available crystallographic data of sodium salicylate so far. Specifically, geometry optimization and vibrational mode calculation were carried out using two different methods, the Becke-3-Lee-Yang-Parr (B3LYP) functional [25] and the second-order Møller–Plesset perturbation theory (MP2) [26], with the 6-311+G (d, p) Gaussian basis set. These two methods were selected for calculations since they could achieve accurate prediction of molecular structures and intramolecular vibrations [10, 27]. The maximum force between atoms converged to better than 10^{-5} eV/Å, and the maximum atom displacement converged to 10^{-5} Å.

Results and discussion. The THz absorption spectra of salicylic acid and sodium salicylate measured at room temperature (RT) are shown in Fig. 2. Distinct spectral differences can be observed, indicating that salicylic acid and sodium salicylate can be easily distinguished from their characteristic THz spectra. Specifically, as listed in Table 1, the THz spectrum of salicylic acid shows six absorption peaks at the following frequencies: 1.11, 1.39, 1.63, 1.84, 2.09, and 2.28 THz. Among these absorption peaks, the highest-intensity peak locates at 2.28 THz, and its shoulder peak lies at 2.09 THz, the remaining four absorption peaks are medium-intensity. In previous studies on salicylic acid, two absorption peaks presented at 2.28 THz (76 cm^{-1}) and 2.70 THz (90 cm^{-1}) [12] and four absorption peaks at 1.11 THz (37 cm^{-1}), 1.38 THz (46 cm^{-1}), 2.07 THz (69 cm^{-1}) and 2.25 THz (75 cm^{-1}) [14]. Our measurements detected all the absorption peaks below 3.6 THz, although it is difficult to declare the existence of the absorption peak at 2.70 THz. The absorption peaks at 1.63 and 1.84 THz in this paper are reported for the first time. As for sodium salicylate, four discernible absorption peaks lower than 3.6 THz were detected, including two high-intensity peaks located at 0.40 and 1.89 THz, a low-intensity peak appearing at 1.05 THz, and a broad absorption band around 2.98 THz. Moreover, the three absorption features, 1.05, 1.89, and 2.98 THz, are reported for the first time.

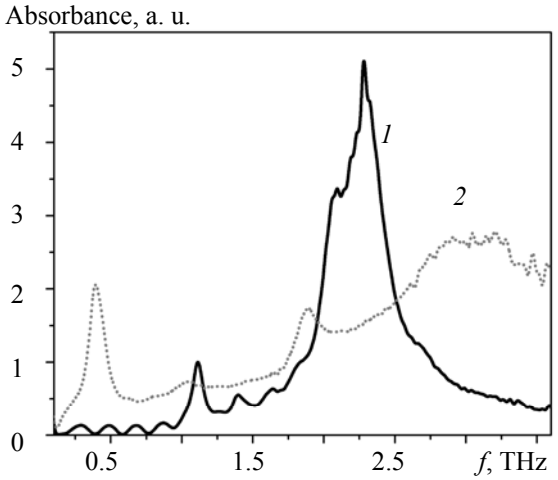

Fig. 2. The measured absorption spectra of salicylic acid (1) and sodium salicylate (2) in the range of 0.1–3.6 THz.

TABLE 1. The Measured Absorption Features (THz) of Salicylic Acid and Sodium Salicylate

Salicylic acid	Sodium salicylate
–	0.40
1.11	1.05
1.39	–
1.63	–
1.84	1.89
2.09	–
2.28	–
–	2.98

Accurate geometric structures are essential to assure high-quality reproduction of vibrational spectra. Generally, simulated geometric structures are evaluated by the root-mean-squared deviations (RMSDs) of the simulated bond lengths and bond angles compared with those determined by crystallographic measurements. Here, the optimized molecular geometric parameters of salicylic acid are summarized in Table 2. The RMSDs of the bond lengths and bond angles are 0.011 Å and 0.3° respectively, demonstrating high-quality molecular structural reproduction achieved by the solid-state DFT calculations. Also, such geometric structural reproduction is adequate for accurately calculating THz spectra of molecular crystals according to the previous studies [19, 27, 28].

TABLE 2. The Optimized Molecular Geometric Parameters of Salicylic Acid

Chemical bond	Bond length, Å		Chemical bond	Bond angle, degree	
	Experiment	Calculation		Experiment	Calculation
C_1–C_2	1.403	1.417	C_1–C_2–C_3	119.4	119.2
C_2–C_3	1.404	1.405	C_2–C_3–C_4	121.3	120.1
C_3–C_4	1.377	1.372	C_3–C_4–C_5	120.5	121.0
C_4–C_5	1.408	1.384	C_4–C_5–C_6	119.5	119.5
C_5–C_6	1.364	1.387	C_5–C_6–C_1	121.3	121.1
C_3–H_{12}	1.067	1.083	C_6–C_1–C_2	119.1	119.0
C_4–H_{13}	1.067	1.083	C_7–O_8–H_{16}	112.4	112.5
C_5–H_{14}	1.033	1.080	O_8–C_7–C_1	116.0	116.8
C_6–H_{15}	1.075	1.081	O_9–C_7–C_1	123.0	121.0
C_7–C_1	1.468	1.451	O_{10}–C_2–C_1	122.8	121.3
C_7–O_8	1.300	1.220	H_{11}–O_{10}–C_2	107.6	108.2
O_8–H_{16}	0.986	1.014	H_{12}–C_3–C_2	116.0	118.6
O_9–C_7	1.231	1.175	H_{13}–C_4–C_3	119.1	119.2
O_{10}–C_2	1.360	1.246	H_{14}–C_5–C_6	119.3	120.5
O_{10}–H_{11}	0.954	0.979	H_{15}–C_6–C_1	116.6	118.4
RMSD	–	0.011	RMSD	–	0.3

The unit cell of salicylic acid consists of four molecules with 64 atoms containing 189 optical modes ($47A_u + 46B_u + 48B_g + 48A_g$). Among these optical modes, 168 optical modes belong to intramolecular vibrations, whereas the other 21 optical modes ($5A_u + 4B_u + 6B_g + 6A_g$) arise from intermolecular interactions. Because the space group of salicylic acid is $P2_1/a$, the optical modes with A_u and B_u symmetries are infrared active, which can be measured by THz-TDS.

To analyze the origin of the measured absorption features, the calculated vibrational modes of salicylic acid and their descriptions are listed in Table 3. The description of the vibrational mode came from a visual inspection of the atomic displacements and the primary contributions to the vibrational mode character. It is clear that the calculated vibrational modes of salicylic acid show a good qualitative agreement with the measured absorption features according to the RMSD value of 0.05. Specifically, the DFT calculations reveal six infrared-active vibrational modes ($3A_u + 3B_u$) below 3.6 THz: five intermolecular (one rotation, two butterfly and two cogwheel) modes, and one intramolecular mode (twisting of Ph-COOH). The calculated mode at 1.12 THz is responsible for the measured feature at 1.11 THz, while the measured features at 1.39 and 1.63 THz can be assigned to the calculated modes at 1.50 and 1.59 THz, respectively. Moreover, the two

measured features at 1.84 and 2.09 THz can be attributed to the two calculated modes at 1.82 and 2.25 THz, respectively. Moreover, the strongest absorption feature at 2.28 THz may originate from the calculated mode at 2.48 THz.

It should be pointed out that, although the dispersion-corrected DFT calculations provide better qualitative reproduction of the absorption features, frequency discrepancies between the measured features and the calculated modes still exist, indicating that long-range intermolecular interactions also play an important role in the low-frequency vibrational modes of solid-state compounds.

The molecular structure and optimized molecular geometries of sodium salicylate are shown in Fig. 3 and Table 4, respectively. The bond lengths and bond angles obtained from the B3LYP calculation are quite similar to those obtained from the MP2 calculation. Specifically, the discrepancies between most of the bond lengths calculated by B3LYP and MP2 are less than 0.012 Å. As for the bond angles, the largest discrepancy is less than 1.8°. Although the bond-length discrepancies of O_8^-–Na_{16}^+ and O_9^-–Na_{16}^+ are 0.064 Å and 0.065 Å, respectively, both the bond-angle discrepancies of C_7–O_8^-–Na_{16}^+ and C_7–O_9^-–Na_{16}^+ are less than 0.3°.

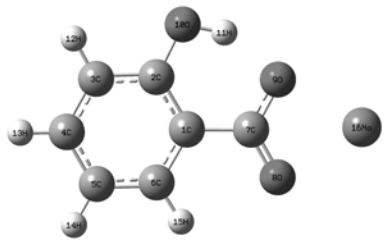

Fig. 3. The molecular structure and atom labeling of sodium salicylate.

TABLE 3. The Assignment of Measured Features and Calculated Modes for Salicylic Acid

Experiment, THz	Calculation		
	Frequency, THz	Infrared intensity, km/mol	Mode description
1.11	1.12	5.61	Rotation along *c* axis
1.39	1.50	5.37	Butterfly of dimers
1.63	1.59	0.84	Butterfly of dimers
1.84	1.82	1.49	Cogwheel of dimers
2.09	2.25	9.38	Cogwheel of dimers
2.28	2.48	13.99	Ph-COOH twisting
RMSD	0.05	–	–

TABLE 4. The Optimized Molecular Geometries of Sodium Salicylate

Bond	Bond length, Å		Bond	Bond angle, degree	
	B3LYP	MP2		B3LYP	MP2
C_1–C_2	1.413	1.406	C_1–C_2–C_3	119.8	120.0
C_2–C_3	1.405	1.400	C_2–C_3–C_4	121.1	120.6
C_3–C_4	1.392	1.397	C_3–C_4–C_5	119.9	119.9
C_4–C_5	1.398	1.397	C_4–C_5–C_6	119.0	119.4
C_5–C_6	1.393	1.396	C_5–C_6–C_1	122.4	121.5
C_3–H_{12}	1.089	1.086	C_6–C_1–C_2	117.8	118.7
C_4–H_{13}	1.087	1.083	C_7–O_8^-–Na_{16}^+	87.7	87.4
C_5–H_{14}	1.056	1.053	C_7–O_9^-–Na_{16}^+	88.0	87.7
C_6–H_{15}	1.084	1.083	O_8–C_7–C_1	118.1	118.0
C_7–C_1	1.506	1.504	O_9–C_7–C_1	120.0	118.5
C_7–O_8	1.280	1.283	O_{10}–C_2–C_1	120.5	118.7
O_8^-–Na_{16}^+	2.194	2.258	H_{11}–O_{10}–C_2	108.5	108.0
O_9^-–Na_{16}^+	2.191	2.256	H_{12}–C_3–C_2	116.0	116.4
O_9–C_7	1.272	1.276	H_{13}–C_4–C_3	119.5	119.5
O_{10}–C_2	1.365	1.377	H_{14}–C_5–C_6	120.4	120.3
O_{10}–H_{11}	0.967	0.967	H_{15}–C_6–C_1	116.6	117.7

Therefore, the molecular structure simulation of sodium salicylate has been done successfully. Moreover, by comparing the molecular geometries of sodium salicylate and salicylic acid, it is easy to find out that the bond lengths and bond angles of the benzene ring in sodium salicylate are very close to those in salicylic acid. However, the bond lengths of C_7–C_1, C_7–O_8 and C_7–O_9 of sodium salicylate exhibit larger differences at least 0.017 Å from those of salicylic acid. A similar phenomena can also be found in the bond angles of O_8–C_7–C_1 and O_9–C_7–C_1 with differences larger than 2°. It is known that the sodium atom in the carboxyl group of the sodium salicylate molecule substitutes the hydrogen atom in the carboxyl group of the salicylic acid molecule, and the ionic bond between COO^- and Na^+ is formed, leading to the electron density redistribution of COO^-. This could be the reason that the bond lengths and bond angles of COO^- in the sodium salicylate molecule show larger differences from those in the salicylic acid molecule. Moreover, the intermolecular hydrogen bond (O–H···O) in salicylic acid dimers is destroyed by the ionic bond formed in the sodium salicylate molecule, leading to the rearrangement of molecules and the change of intermolecular interactions in the crystal. The intra- and intermolecular structural differences between salicylic acid and sodium salicylate result in their distinctive THz spectral features.

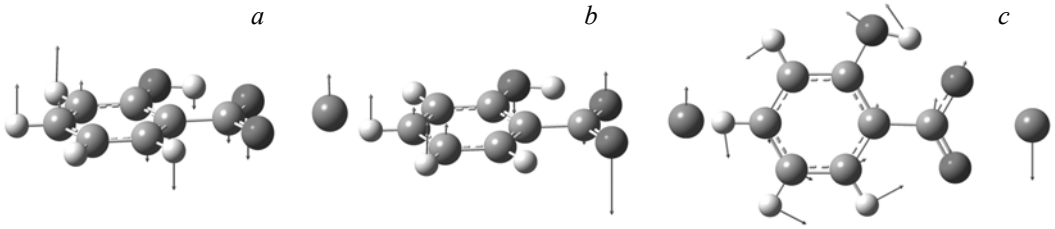

Fig. 4. The intramolecular vibrational modes of sodium salicylate (MP2 calculations): a) 1.29 THz, bending of Ph-COONa; b) 1.83 THz, twisting of Ph-COONa; c) 3.12 THz, rocking of Ph-COONa.

Table 5 lists the measured spectral features and calculated vibrational modes of sodium salicylate. Both B3LYP and MP2 calculations based on the isolated molecule show three infrared-active intramolecular modes, namely bending, twisting, and rocking of Ph-COONa, as illustrated in Fig. 4. Specifically, the B3LYP calculations present the vibrational modes at 0.83, 2.23, and 4.18 THz, while the MP2 calculations provide the vibrational modes at 1.29, 1.83, and 3.12 THz. According to the RMSDs, it is obvious that the frequency discrepancies between the measured features and the calculated modes obtained by the MP2 calculations are smaller than those obtained by the B3LYP calculations. The MP2 calculations considered the second-order correction of electronic correlation energy [26], which may lead to the better reproduction of the measured intramolecular vibrational modes. Moreover, although there are no available crystallographic data of sodium salicylate for calculation based on the periodic system, the MP2 calculations based on the isolated molecule have also achieved a good qualitative agreement with the measured intramolecular vibrations by a very small RMSD value. Based on the MP2 calculations, the measured absorption features at 1.05, 1.89, and 2.98 THz can be assigned to the calculated vibrational modes at 1.29, 1.83, and 3.12 THz, respectively. Moreover, the absorption feature at 0.40 THz may originate from intermolecular vibration, since the MP2 calculations based on the isolated molecule show that there is no intramolecular vibrational mode around 0.40 THz.

TABLE 5. The Assignment of Measured Features and Calculated (MP2 and B3LYP) Modes (THz) for Sodium Salicylate

Experiment	MP2	B3LYP	Mode description
1.05	1.29	0.83	Bending of Ph-COONa
1.89	1.83	2.23	Twisting of Ph-COONa
2.98	3.12	4.18	Rocking of Ph-COONa
RMSD	0.09	0.42	–

Conclusion. The THz absorption spectra (0.1–3.6 THz) of salicylic acid and sodium salicylate are measured by broadband THz-TDS at room temperature. The absorption features at 1.63 and 1.84 THz of salicylic acid as well as the absorption features at 1.05, 1.89, and 2.98 THz of sodium salicylate are reported for the first time to the best of our knowledge. Distinct THz spectral differences between salicylic acid and

sodium salicylate are also observed, implying that they can be easily distinguished from their THz characteristic spectra. Moreover, by comparing the molecular structures of salicylic acid and sodium salicylate, it is found that the ionic bond of sodium salicylate affects not only the bond lengths and bond angles of covalent bonds but also the intermolecular interactions in the unit cell, which results in the distinct THz spectral differences.

Moreover, the solid-state DFT simulations of salicylic acid give high-quality reproduction of the molecular structures and the measured absorption features. According to the calculations, the absorption features of salicylic acid mainly come from intermolecular interactions, except for the feature at 2.28 THz. Furthermore, the theoretical calculations of sodium salicylate reveal that the absorption features mainly originate from intramolecular vibrations, except for the absorption feature at 0.40 THz. These results are beneficial for understanding the effect of molecular structure differences on the low-frequency vibrational modes, which is also advantageous for distinguishing chemicals and pharmaceuticals with similar structures.

Acknowledgment. This work was financially supported by the National Natural Science Foundation (Grant No. 61675230), the 'Hundreds of Talents Programs' of the Chinese Academy of Sciences (Grant No. J08-029), the Innovative Project of the Chinese Academy of Sciences (Grant No. YYYJ-1123-4), and the CAS/SAFEA International Partnership Program for Creative Research Teams.

REFERENCES

1. G. Davies, A. D. Burnett, W. H. Fan, E. H. Linfield, J. E. Cunningham, *Mater. Today*, **11**, 18–26 (2008).
2. J. Hooper, E. Mitchell, C. Konek, J. Wilkinson, J. Wilkinson, *Chem. Phys. Lett.*, **467**, 309–312 (2009).
3. F. Zhang, O. Kambara, K. Tominaga, J. I. Nishizawa, T. Sasaki, H. W. Wang, M. Hayashi, *RSC Adv.*, **4**, 269–278 (2014).
4. Z. P. Zheng, W. H. Fan, *J. Biol. Phys.*, **38**, 405–413 (2012).
5. M. D. King, W. Ouellette, T. M. Korter, *J. Phys. Chem. A*, **115**, 9467–9478 (2011).
6. D. Suhandy, T. Suzuki, Y. Ogawa, N. Kondo, H. Naito, T. Ishihara, W. Liu, *Eng. Agric. Environ. Food*, **5**, 90–95 (2012).
7. K. Shiraga, T. Suzuki, N. Kondo, J. D. Baerdemaeker, Y. Ogawa, *Carbohydr. Res.*, **406**, 46–54 (2015).
8. M. Song, F. Yang, L. Liu, L. Shen, P. Hu, F. Han, *J. Nanosci. Nanotechnol.*, **16**, 12208–12213 (2016).
9. M. T. Ruggiero, T. Bardon, M. Strlic, P. F. Taday, T. M. Korter, *J. Phys. Chem. A*, **118**, 10101–10108 (2014).
10. Z. P. Zheng, W. H. Fan, H. Yan, J. Liu, L. M. Xu, *Spectrosc. Spect. Anal.*, **33**, 582–585 (2013).
11. S. Saito, T. M. Inerbaev, H. Mizuseki, N. Igarashi, Y. Kawazoe, *Jpn. J. Appl. Phys.*, **45**, 4170–4175 (2006).
12. M. Boczar, Ł. Boda, M. J. Wójcik, *J. Chem. Phys.*, **124**, 084306 (2006).
13. N. Laman, S. S. Harsha, D. Grischkowsky, *Appl. Spectrosc.*, **62**, 319–326 (2008).
14. M. Takahashi, Y. Ishikawa, H. Ito, *Chem. Phys. Lett.*, **531**, 98–104 (2012).
15. D. J. Bakker, A. Peters, V. Yatsyna, V. Zhaunerchyk, A. M. Rijs, *J. Phys. Chem. Lett.*, **7**, 1238–1243 (2016).
16. J. Hisazumi, T. Watanabe, T. Suzuki, N. Wakiyama, K. Terada, *Chem. Pharm. Bull.*, **60**, 1487–1493 (2012).
17. S. J. Clark, M. D. Segall, C. J. Pickard, P. J. Hasnip, M. I. Probert, K. Refson, M. C. Payne, *Z. Kristallogr.*, **220**, 567–570 (2005).
18. J. P. Perdew, K. Burke, M. Ernzerhof, *Phys. Rev. Lett.*, **77**, 3865–3868 (1996).
19. Z. P. Zheng, W. H. Fan, H. Li, J. Tang, *J. Mol. Spectrosc.*, **296**, 9–13 (2014).
20. M. T. Ruggiero, J. Gooch, J. Zubieta, T. M. Korter, *J. Phys. Chem. A*, **120**, 939–947 (2016).
21. A. Tkatchenko, M. Scheffler, *Phys. Rev. Lett.*, **102**, 073005 (2009).
22. L. Kleinman, D. M. Bylander, *Phys. Rev. Lett.*, **48**, 1425–1428 (1982).
23. R. A. Evarestov, V. P. Smirnov, *Phys. Rev. B*, **70**, 155–163 (2004).
24. W. Cochran, *Acta Crystallogr.*, **6**, 260–268 (1953).
25. A. D. Becke, *J. Chem. Phys.*, **98**, 5648–5652 (1993).
26. M. Head-Gordon, J. A. Pople, M. J. Frisch, *Chem. Phys. Lett.*, **153**, 503–506 (1988).
27. J. Dash, S. Ray, K. Nallappan, V. Kaware, N. Basutkar, R. G. Gonnade, B. Pesala, *J. Phys. Chem.*, A **119**, 7991–7999 (2015).
28. M. Takahashi, Y. Ishikawa, *Chem. Phys. Lett.*, **642**, 29–34 (2015).